PERIODICA POLYTECHNICA SER. EL. ENG. VOL. 41, NO. 2, PP. 147-166 (1997)

ANALYSIS AND IMPROVEMENT OF DETERMINISTIC URBAN WAVE PROPAGATION MODELS

Zoltán SÁNDOR, Tamás CSABA, Zoltán SZABÓ and Lajos NAGY

Department of Microwave Telecommunications
Technical University of Budapest
H-1521 Budapest, Hungary
tel.: 463-4218; fax: 463-3289
email: d-sandor@ nov.mht.bme.hu

Received: March 26, 1997

Abstract

An error analysis of the COST 231 Walfish-Ikegami model [1] proposed for urban area and the demonstration of a 3 dimensional deterministic wave propagation model are made in this paper. First the sensitivity of the COST 231 model to the uncertainty of the building parameters is analyzed and a modification in the application of the model that reduces the error caused by the irregular building structure is performed. The effect of the building database accuracy is also shown. The need for a more precise propagation model appears, and the first results from a 3D deterministic model based on the Uniform Theory of Diffraction are presented . The validity of the approximation in the calculation of the diffraction coefficients and the effect of the slope diffraction are investigated, and results of measurements of material parameters necessary for the model are presented. The calculations are assessed by measurements at 900 MHz on a suitable part of Budapest.

Keywords: mobile communications, propagation models, material parameters.

Introduction

The prediction of the path loss is a very important step in planning the cellular mobile systems. The semiempirical COST 231 WALFISH-IKEGAMI model [1] developed for predicting the path loss in urban environment is based on the theoretical works of WALFISH and BERTONI [2] and IKEGAMI [3] and has included empirical correction factors introduced by the COST 231.

In the first part of this paper the error introduced by the uncertainty of the model parameters in the path loss prediction is examined, by other words how accurate the parameters have to be in order that the predicted path loss prediction achieve a desired accuracy. This problem appears during the construction of databases containing data on the building structure, or in the application of the model with mean parameter values. A modification in the application of the COST 231 model ensuring better appli-

cability on wide streets and squares and where the building height varies along the propagation path is introduced.

In the second part of the paper the vertical plane component of the 3D model based on the Uniform Theory of Diffraction (UTD) is described. The measured values of the parameters of the building materials characteristic to the test area are also presented.

In the third part a comparison between measurements and prediction at 900 MHz on a selected area of Budapest is made, showing the applicability of the COST 231 Walfish–Ikegami model, the reduction of the prediction error with the modification of the model, the effect of the database accuracy and the results of the vertical propagation model.

Error Analysis of the COST 231 Model

The model assumes a rectangular street grid with equidistantly spaced buildings as half screens having the same height and can be applied in the following range of the parameters:

- frequency range , f = 800–2000 MHz
- base station (BS) antenna height, h_b = 4–50 m
- mobile station (MS) antenna height, h_m = 1–3 m
- distance between the BS–MS, d=0.02–5 km

The different parameters used by the model are shown on *Fig. 1*:

- adjacent building distance, b
- street width, w
- building height, h_{roof}
- street orientation, fi.

The COST 231 Walfish–Ikegami model gives the basic path loss L_b and it is composed of three terms:

$$L_b = \begin{cases} L_0 + L_{rts} + L_{msd} \\ L_0 \qquad\qquad \text{for} \qquad L_{rts} + L_{msd} \leq 0, \end{cases} \tag{1}$$

where L_0 represents the free space loss, L_{rts} the 'roof-top-to-street diffraction and scatter loss' and the term L_{msd} the 'multi-screen loss'. The free space loss is given by

$$L_0 = 32.4 + 20 \lg d^{[km]} + 20 \lg f^{[MHz]}. \tag{2}$$

The roof-to-street diffraction and scatter loss is

$$L_{rts} = -16.9 - 10 \lg w^{[m]} + 10 \lg f^{[MHz]} + 20 \lg \Delta h_m^{[m]} + L_{ori}, \tag{3}$$

where

$$L_{ori} = \begin{cases} -10 + 0.354 * fi^{[\mathrm{deg}]} \text{ for } 0 \leq \mathrm{fi} \leq 35°, \\ 2.5 + 0.075 * \left(fi^{[\mathrm{deg}]} - 35\right) \text{ for } 35° \leq fi \leq 55°, \\ 4.0 - 0.114 * \left(fi^{[\mathrm{deg}]} - 55\right) \text{ for } 55° \leq fi \leq 90°, \end{cases} \tag{4}$$

$$\begin{cases} \Delta h_m = \mathrm{h_{roof}} - \mathrm{h_m} \\ \Delta h_b = \mathrm{h_b} - \mathrm{h_{roof}} \end{cases} \tag{5}$$

The multi-screen diffraction loss is

$$L_{msd} = L_{bsh} + k_a + k_d \lg d[m] + k_f \lg f^{[MHz]} - 9 \lg b^{[m]} \tag{6}$$

where

$$L_{bsh} = \begin{cases} -18lg\left(1 + \Delta h_b^{[m]}\right) \text{ for } \mathrm{h_b} > h_{roof} \\ 0 \text{ for } \mathrm{h_b} \leq h_{roof} \end{cases} \tag{7}$$

$$k_a = \begin{cases} 54 & \text{for } h_b > h_{roof} \\ 54 - 0.8\Delta h_b^{[m]} & \text{for } d \geq 0.5 \text{ km} \\ & \text{and} \quad h_b \leq h_{roof} \\ 54 - 0.8(\Delta h_b^{[m]} * d^{[km]}/0.5) & \text{for } d < 0.5 \text{ km} \\ & \text{and} \quad h_b \leq h_{roof}, \end{cases} \tag{8}$$

and

$$k_d = \begin{cases} 18 \quad \text{for} \quad h_b > h_{roof} \\ 18 - 15\frac{\Delta hb}{h_{roof}} \quad \text{for} \quad h_b \leq h_{roof} \end{cases} \tag{9}$$

and

$$k_f = -4 + \begin{cases} 0.7\left(\frac{f^{[MHz]}}{925} - 1\right) \text{ for medium-sized cities and} \\ \qquad\qquad \text{centers with mod. tree density,} \\ 1.5\left(\frac{f^{[MHz]}}{925} - 1\right) \text{ for metropolitan centers.} \end{cases} \tag{10}$$

For the case when information on the building structure are not available default values from the following range are recommended:

b= 20.. 50 m;

$w = b/2$;

h_{roof}=3 m *{number of floors} +roof;

roof= $\begin{cases} 3 \text{ m , pitched} \\ 0 \text{ m , flat} \end{cases}$ fi=90°.

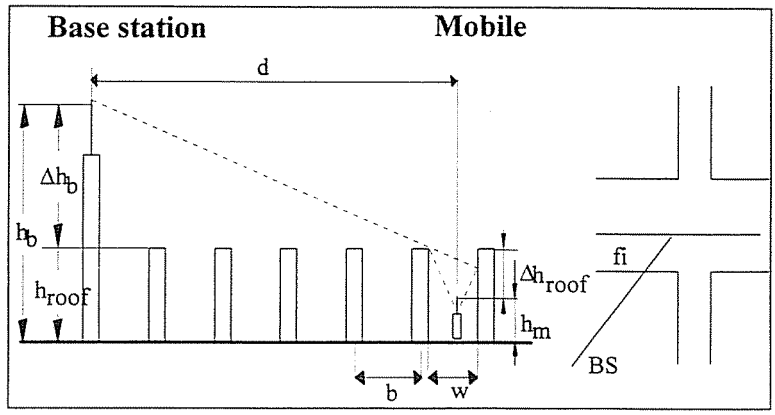

Fig. 1. The parameters of the COST 231 W-I. model

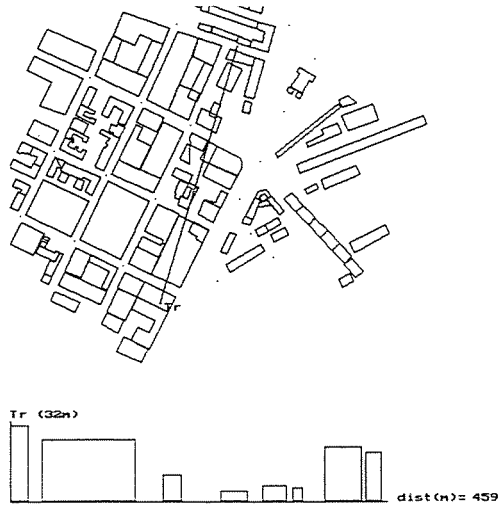

Fig. 2. The building database

The influence of the imprecision of the parameters can be estimated from the equations of the model [1].

Since with the exception of the h_{roof} the parameters of the model are independent of the distance d, in order that the numerical results are more general the average path loss $< L >$ was computed in steps of 10 m in the whole range of the BS–MS distances of 0.02-5 km. In the case of the error introduced by the h_{roof} the averaging of the path loss was made between 0.5 and 5 km.

The numerical analysis of the error was performed around the values of $b = 50$ m, $w = 25$ m , $h_{roof} = 26$ m that represent the mean values

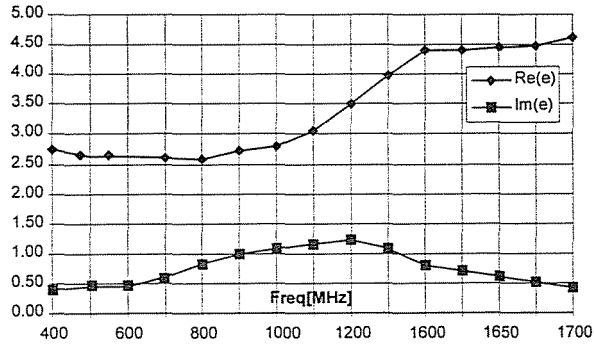

Fig. 3. Material parameters of a brick sample

characteristic to the test area. The other parameters around which the error is computed are h_b=32 m, h_m =1.5 m including a street orientation of fi=80°, a frequency of f=943 MHz; urban area with metropolitan city characteristic to the test area were assumed.

The building distance b is included in term L_{msd} given by *Eq.* (6) and its increase means a 9 dB/dec decrease in the path loss. In the numerical presentation the influence of b was examined between 5 and 50 m because these are the mean values practically possible for the given area. *Fig 4* presents the average path loss $< L >$ versus b with h_{roof} as a parameter. It can be seen from the figure that because of the independence of the parameters the curves are in parallel. Results of calculations with various parameters including $b \neq 50$ m are collected in *Table 1*. It can be seen from *Table 1* that for $b = 50$–10 m and $b = 50$+15 m the deviation of the path loss from that of the $b = 50$ m condition is around 1 dB.

The error introduced by the street width w can be determined from the *Eq.* (3) giving the term L_{rts}. In this case the decrease of the path loss is 10 dB/dec with the increase of w, which means that a smaller uncertainty of w than that of b introduces the same error. *Fig. 5* shows the average path loss, $< L >$ versus w with h_{roof} as a parameter. Similar to the previous case the curves are in parallel. *Table 1* shows that for $w = 25$–5 m and $w =$ 25+5 m the deviation of the path loss from that of the $w = 25$ m condition is around 1 dB.

The excess path loss L_{ori} represents the influence of the street orientation, fi and it is given by *Eq.* (4) in three different terms and for which reason the model should be applied carefully when fi is around 350 and 550 because the resulted error can be significant. *Fig. 6* shows the averaged path loss $< L >$ versus fi with b as parameter. It can be observed from *Fig. 6* the parallel curves owing to the independence of the parame-

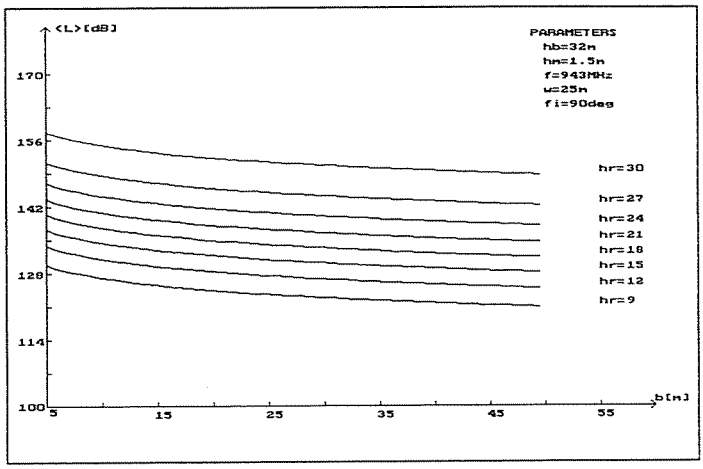

Fig. 4. The influence of the building distance

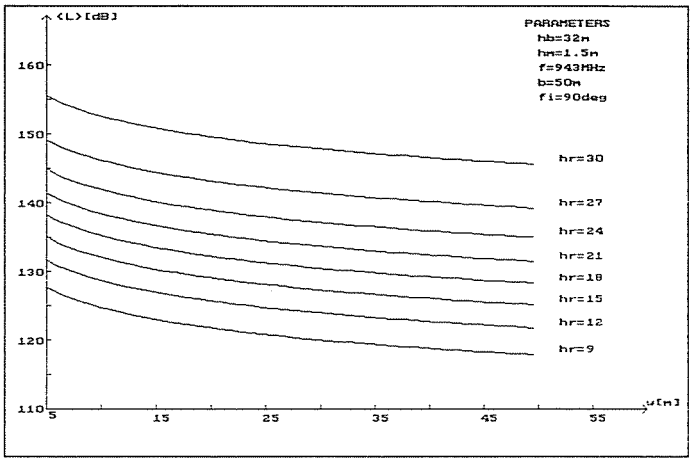

Fig. 5. The influence of the street width

ters, and the piecewisely linear character due to the above mentioned three different terms of L_{ori}. *Table 1* shows that a deviation of fi by $\pm 9^\circ$ around $fi = 80^\circ$ introduces an error by about 1 dB.

Figs. 4, 5, 6 also show that the averaged path loss curves are not linear, by other words the error introduced by the uncertainty of the parameters (b, w, fi) depends also on the magnitude of the parameters, which corresponds to the reality.

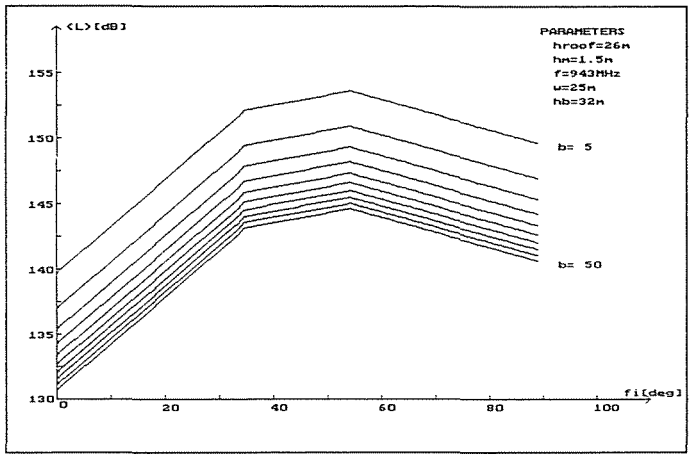

Fig. 6. The influence of the street orient

The influence of the building height appears in different equations of the COST 231 Walfish – Ikegami model [3,6,8,9], and can be observed that in contrast to the other parameters the error introduced by the h_{roof} depends on the h_b and in the case of $d < 0.5$ km and when $h_b <= h_{roof}$ it depends also on d, which corresponds to the practical situation. For this reason, in the numerical analysis of the error introduced by the h_{roof} the computation of the average path loss was done between $d = 0.5$ km and 5 km. Because at the test area mean values out of this range are not very probable, the building height was computed between h_{roof} =9 m to 30 m. *Fig. 7* shows the average path loss, $< L >$ versus h_{roof} with h_b as parameter. It can be observed from *Fig. 7* that the case when h_{roof} has the same value as h_b represents a relative big error source in the application of the model.

Table 1 shows that a deviation of h_{roof} by 0.7 and 0.6 m around the mean $h_{roof} = 26$ m value introduces an error in the path loss of approx. 1 dB. *Fig. 8* shows the path loss, L versus h_{roof} curves with the MS–BS distance, d as parameter for $d <=0.5$ km, where because of the dependence of the h_{roof} on d shown also by *Eq.* (9) the curves are no longer in parallel. Similar curves are presented in [4]. The error introduced by the uncertainty of the h_{roof} can be read from *Fig 7* for any practically possible value of the other parameters with the condition of $d >0.5$ km or $d < = 0.5$ km and $h_b > h_{roof}$. In case when $d <=0.5$ km and $h_b <=h_{roof}$ the error has to be examined separately for different values of the distance d between the BS and MS.

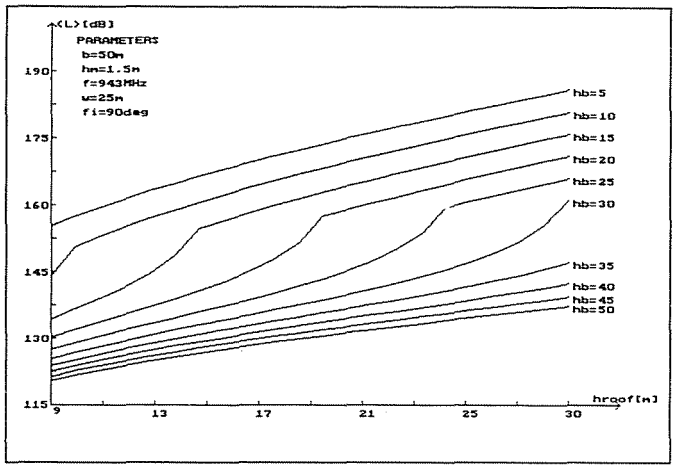

Fig. 7. The influence of the building height

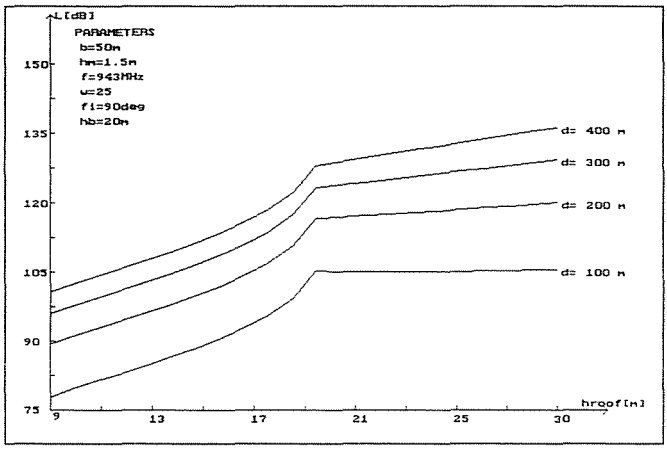

Fig. 8. The influence of the building height ($d < 0.5$ km)

With the above presented figures the error introduced by the uncertainty of the parameters can be determined. Usually in the application of the model not only one but all of the parameters are in error to some degree so the aggregate error has to be analysed. The aggregate error can be obtained from *Fig.4 – Fig. 8* and for a specific parameter combination is also given in *Table 1*, showing that the aggregate error results as the sum of the partial errors, which is explained by the independence of the param-

Table 1
Uncertainty of the parameters

	w[m]	roof[m]	fi[deg]	$< L >$[dBm]	ε[dB]
50	25	26	80	145.64	
65	25	26cc	80	144.61	1.03
50	30	26	80	144.84	0.8
50	20	26	80	146.6	−0.96
50	25	26.6	80	146.55	−0.91
50	25	25.3	80	144.64	1
50	25	26	71	146.66	−1.02
50	25	26	89	144.61	1.03
65	30	25.3	89	141.80	3.84
40	20	26.6	71	149.41	−3.77

eters. It should be mentioned that the above error analysis refers to the erros introduced by the uncertainty of the building parameters, beside which other errors caused by the nature of the model are present. Therefore, the above analysis gives a low boundary for the path loss error.

Modification in the Application of the COST 231 Model

As was mentioned the COST 231 Walfish–Ikegami model assumes regular building structure with rectangular street grid and buildings having the same height. However, the above assumptions in the majority of the cities are not satisfied and in this case the model gives a relative large prediction error.

Using a digitised database containing the building structure the fluctuation of the building heights and building distance on this area of Budapest can be seen (*Fig. 2*).

Fig 2 shows a segment between the BS and MS on the test area for a given position of the MS. Because of the variation of the building heigth along the radio path the calculation of the average building height taking into consideration all of the buildings between the MS and BS can conduct to relative large errors, because the small buildings have not a dominant effect on the wave propagation but reduce the average building height. For this reason in the calculation of the mean building height the small buildings will not be taken into account. First the average h_{favg} including all of the buildings between the MS and BS is determined after that the buildings having a smaller height than the resulted average by 20% are excluded and the calculation of the average height is repeated with the

remaining buildings, obtaining in this way the mean value, h_{roof}:

$$h_{fav.} = \frac{\sum_{i=1}^{n} h_i}{n}, \tag{11}$$

where

h_i – the height of the building on the radio path,
n – the total number of the buildings along the radio path.
The average building height results as

$$h_{roof} = \frac{\sum_{j=1}^{n-p} h_j}{n-p}, \tag{12}$$

where

h_j – the height of the buildings exceeding the first average value,

p – the number of buildings along the radio path having height below the first average by 20%.

Another observation that can be made is that using the width w of the street on which the mobile is located conducts to errors in the case of road intersections or empty squares, where the street width differs from w. For this reason in the case when the distance between the MS assumed to be situated in the middle of the street and the building in the vicinity of the MS exceeds by 10% the street width $w1$ the exact distance between the MS and the building $w2$ is considered.

As known, the term L_{msd} in the COST 231 model given by *Eq.* (6) is derived from the model of WALFISH and BERTONI [2] considering the buildings as equidistantly spaced knife edges having the same height. The term L_{rts} is given by the model of IKEGAMI [3] based on geometrical optics and considering the effect of the buildings near the MS.

If $h_{roof}1$ represents the average height of the buildings along the radio path and $h_{roof}2$ the value of the building height in the vicinity of the MS, for the case when $h_{roof}2 > h_{roof}1$ the value $h_{roof}2$ should be used in the terms of the COST 231 model derived from the Ikegami model L_{rts} in order to taking into consideration better the effect of the building height.

Since the COST 231 model presents large prediction errors in the cases when its assumptions are not satisfied and the suggested improvement can reduce this error only to some degree, the need for a more precise 3D model appears.

The 3D Model

To achieve a better prediction we used an other model based on the UTD (Uniform Theory of Diffraction). In contrary to the previously mentioned methods this one applies the geometrical optics.

While working with UTD we choose an edge fixed coordinate system, ($\hat{\beta}'0, \hat{\phi}', \hat{\beta}0, \hat{\phi}$ are parallel or perpendicular unit vectors to incident and the diffraction plane, and $\hat{s}' = \hat{\phi} \times \hat{\beta}'0$, $\hat{s} = \hat{\phi}' \times \hat{\beta}0$). We are looking for the solution in the form of:

$$\begin{bmatrix} E^d{}_{\beta 0} & (s) \\ E^d{}_{\phi} & (s) \end{bmatrix} = - \begin{bmatrix} D_s & 0 \\ 0 & D_h \end{bmatrix} \begin{bmatrix} E^i{}_{\beta 0'} & (Q) \\ E^i{}_{\phi'} & (Q) \end{bmatrix} A(s', s) e^{-j\beta s},$$

where the incident field component parallel to the incident plane is $E^i{}_{\beta' 0}(Q) = \hat{\beta}'0 * \mathbf{E}^i$ and the perpendicular component is $E^i{}_{\phi'}(Q) = \hat{\phi}' * \mathbf{E}^i$.

The diffraction coefficients can be written as: $D_s(\phi\phi', n, \beta'0) = D_i(\phi - \phi', n, \beta'0) - D_r(\phi, +\phi', n, \beta'0)$, the soft coefficient, $D_h(\phi\phi', n, \beta'0) = D_i(\phi - \phi', n, \beta'0) + D_r(\phi, +\phi', n, \beta'0)$, the hard coefficient.

Keller dealt with this problem thoroughly and his theories are summarized in the literature as GTD (Geometrical Theory of Diffraction). However, his formulas do not give continuous solution on the incident ($\phi = \pi + \phi'$) and diffraction ($\phi = \pi - \phi'$) boundary.

To get rid of these singularities Kouyoumjian and Pathak modified the previous theory and published it under the name of UTD (Uniform Theory of Diffraction). According to the UTD the diffraction coefficients have the following components:

$$D_i(L, \phi - \phi', n, \beta'0) = \frac{e^{-j\pi/4}}{2n\sqrt{2\pi\beta}\sin\beta'0} \Big\{ \cot[\frac{\pi + (\phi - \phi')}{2n}] F[\beta L g^+(\phi - \phi')$$

$$+ \cot[\frac{\pi - (\phi - \phi')}{2n}] F[\beta L g^-(\phi - \phi')\Big\},$$

$$D_r(L, \phi + \phi', n, \beta'0) = \frac{e^{-j\pi/4}}{2n\sqrt{2\pi\beta}\sin\beta'0} \Big\{ \cot[\frac{\pi + (\phi + \phi')}{2n}] F[\beta L g^+(\phi + \phi')$$

$$+ \cot[\frac{\pi - (\phi + \phi')}{2n}] F[\beta L g^-(\phi + \phi')\Big\},$$

where $g^+ = 1 + \cos[(\phi m \phi') - 2n\pi N^+]$ and $g^- = 1 + \cos[(\phi m \phi') - 2n\pi N^-]$.

In this expression N^+, N^- are the positive, negative integers or zero, which satisfies most closely the following equations:

$$2n\pi N^+ - (\phi m \phi') = +\pi \quad \text{for} \quad g^+,$$

$$2n\pi N^- - (\phi m\phi') = -\pi \quad \text{for} \quad g^-.$$

L in general is: $\frac{s(p_e^i+s)pi1pi2\sin^2\beta'0}{p_e^i(pi1+s)(pi2+s)}$ where $pi1, pi2$ are the incident wave front radius in the point of the diffraction and p_e^i denotes the same in an edge fixed coordinate system. For some special cases, however, the equation looks simpler:

$s\sin^2\beta'0$ for plane wave,

$\frac{s\sin\beta 0 s'\sin\beta'0}{s\sin\beta 0 + s'\sin\beta'0}$ for cylindrical wave,

$\frac{ss'\sin^2\beta'0}{s+s'}$ for the case of spherical incident wave.

The Fresnel transition function (F) is in charge of the continuity of the solution on the boundaries as mentioned. Its most general mathematical form can be written as:

$$F[\beta Lg^+(\phi-\phi')] = 2j\sqrt{\beta Lg^+(\phi-\phi')}e^{+j\beta Lg^+(\phi-\phi')}\int_{\sqrt{\beta Lg^+(\phi-\phi')}}^{\infty} e^{-\tau^2}d\tau$$

$$F[\beta Lg^-(\phi-\phi')] = 2j\sqrt{\beta Lg^-(\phi-\phi')}e^{+j\beta Lg^-(\phi-\phi')}\int_{\sqrt{\beta Lg^-(\phi-\phi')}}^{\infty} e^{-\tau^2}d\tau$$

$$F[\beta Lg^+(\phi+\phi')] = 2j\sqrt{\beta Lg^+(\phi+\phi')}e^{+j\beta Lg^+(\phi+\phi')}\int_{\sqrt{\beta Lg^+(\phi+\phi')}}^{\infty} e^{-\tau^2}d\tau$$

$$F[\beta Lg^-(\phi+\phi')] = 2j\sqrt{\beta Lg^-(\phi+\phi')}e^{+j\beta Lg^-(\phi+\phi')}\int_{\sqrt{\beta Lg^-(\phi+\phi')}}^{\infty} e^{-\tau^2}d\tau$$

The Fresnel integral can be approximated in the following way:

$$\text{if} \quad x > 10 F(x) \cong 1$$

$$\text{if} \quad x < 0.3 F(x) \cong [\sqrt{\pi x} - 2xe^{j\pi/4} - \frac{2}{3}x^2 e^{-j\pi/4}]e^{j(\pi/4+x)},$$

$$\text{if} \quad x > 5.5 F(x) \cong 1 + j\frac{1}{2x} - \frac{3}{4}\frac{1}{x^2} - j\frac{15}{8}\frac{1}{x^3} + \frac{75}{16}\frac{1}{x^4},$$

if $0.3 < x < 5.5$ linear interpolation is used to find $F(x)$.

We also calculated the slope diffraction coefficients, which become significant, when the incident field is small, since this one is proportional to

the first derivative of the field. The diffraction coefficients are the following for soft and hard polarizations, respectively:
for *soft* polarization

$$E_d = \frac{1}{j\beta}\left[\frac{\partial E_i(Q)}{\partial n}\right]\left(\frac{\partial D_s}{\partial \phi'}\right)\sqrt{\frac{pc}{s(pc+s)}}e^{-j\beta s},$$

$$\frac{\partial E_i(Q)}{\partial n} = \frac{1}{s'}\frac{\partial E_i}{\partial \phi'}\Big|_Q,$$

$$\frac{\partial D_s(\phi,\phi',n,\beta' 0)}{\partial \phi'} =$$

$$-\frac{e^{-j\pi/4}}{4n^2\sqrt{2\pi\beta}\sin\beta' 0}\Big\{\left(1/\sin^2\left[\frac{\pi+(\phi-\phi')}{2n}\right]F_s[\beta L g^+(\phi-\phi')\right]$$

$$-1/\sin^2\left[\frac{\pi+(\phi-\phi')}{2n}\right]F_s[\beta L g^-(\phi-\phi')]$$

$$+\left(1/\sin^2\left[\frac{\pi+(\phi+\phi')}{2n}\right]F_s[\beta L g^+(\phi+\phi')]\right.$$

$$\left.-1/\sin^2\left[\frac{\pi+(\phi+\phi')}{2n}\right]F_s[\beta L g^-(\phi+\phi')]\right\}$$

for *hard* polarization

$$H_d = \frac{1}{j\beta}\left[\frac{\partial E_i H_i(Q)}{\partial n}\right]\left(\frac{\partial D_h}{\partial \phi'}\right)\sqrt{\frac{pc}{s(pc+s)}}e^{-j\beta s},$$

$$\frac{\partial H_i(Q)}{\partial n} = \frac{1}{s'}\frac{\partial H_i}{\partial \phi'}\Big|_Q,$$

$$\frac{\partial D_h(\phi,\phi',n,\beta' 0)}{\partial \phi'} =$$

$$-\frac{e^{-j\pi/4}}{4n^2\sqrt{2\pi\beta}\sin\beta' 0}\Big\{\left(1/\sin^2\left[\frac{\pi+(\phi-\phi')}{2n}\right]F_s[\beta L g^+(\phi-\phi')\right]$$

$$-1/\sin^2\left[\frac{\pi-(\phi-\phi')}{2n}\right]F_s[\beta L g^-(\phi-\phi')]$$

$$+\left(1/\sin^2\left[\frac{\pi+(\phi+\phi')}{2n}\right]F_s[\beta L g^+(\phi+\phi')]\right.$$

$$\left.-1/\sin^2\left[\frac{\pi-(\phi+\phi')}{2n}\right]F_s[\beta L g^-(\phi+\phi')]\right)\Big\}$$

where $F_s(x) = 2jx[1 - F(x)]$.

Based on the method of CICHON et al. [9], [10] we constructed our own model. This model is split into three components just like that of the German colleagues.

The first component of the model works in the so-called vertical plane, which contains the transmitter and the receiver and is perpendicular to the ground. Here we computed the diffraction coefficients at each wedge and summarized the diffraction effect in diffraction matrices.

Since an extra diffracting edge might cause 20 dB loss, one of the hardest tasks was to come up with an effective ray tracing algorithm. In order to keep the model manageable, we divided the wedges into two groups. The first consists of the so-called first order obstacles, on which the ray must pass along its way from the transmitter to the receiver. Among these first order obstacles the higher order wedges are located. Additionally to the first order propagation path, routes with one extra diffraction on higher order obstacles contribute as much as 10–20 dB less than the frist order pathto the total. This implies that more than two additional diffractions should not be considered.

We launched a ray from the transmitter to the receiver. We found the first edge, which must be in the path (it does not necessarily have to be the first edge that intersects the receiver-transmitter line). Afterwards from this edge an other ray was launched to the receiver and the process continued recursively until all the first order edges were collected. Among the first order edges the second order edges were differentiated from the third order edges in a similar way as it was done for the first order edges. However, between two first order edges there might be more second order edges, which lead to a multiple propagation.

The transverse plane, which also contains the transmitter–receiver line and perpendicular to the previous mentioned plane helps predict the coverage in situations, where the propagation mainly takes place under the roof top level. In micro cell systems this component becomes extremely important, while in macro cell environment the vertical component alone gives fairly good results.

For the correction of the first two components a third one is introduced. This one searches and calculates the transmission on scattered paths. In order to use a prediction model for real planning purposes, we not only need an accurate method, but also a quick one. Taking the scattered components into consideration the model becomes more complicated and the results do not improve very much [9].

The database is in a vector form. The test area was digitized and each roof is characterized by its height and the corner points (in EOVX,Y coordinates) of the corresponding building.

The results of the vertical plane model were also compared with the measurements. The comparison shows good agreement, but the differences become larger, when propagation on the street level should be taken into consideration. We plan to complete the model with the transverse plane, which will yield even better results.

The measurement of the material parameters needed for the 3D model was performed as described in [11] for the 400–1700 MHz frequency range. The results are presented by *Table 2* and *Fig. 3* showing good agreement with previous measurements reported by the literature.

Comparison between Measurements and Prediction

The Measurements and the Test Area

The measurements were carried out on a relative smooth area of Budapest characterised by inhomogeneous building structure. In the calculation urban environment and metropolitan city were assumed.

A 65° half power beam width directional BS antenna, with an effective radiated power of ERP = 195 W in the main antenna beam direction, which was 320° from North in clockwise was used on the test area shown by *Fig. 9*. The receiver consisted of a modified MS with antenna of 2 dB gain and of $h_m = 1.5$ m height.The measurements were obtained according to [5].

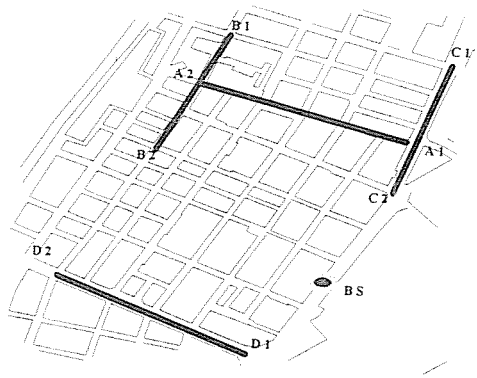

Fig. 9. The test area

As shown by *Fig. 9* four different measuring routes were chosen on the part of the test area for which digitised building database containing the height of the buildings is available. *Fig. 2* shows a part of the test area given by

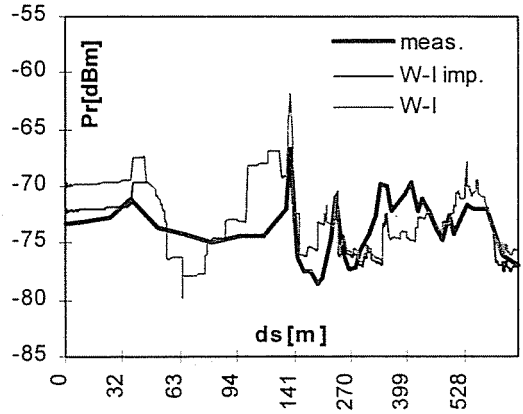

Fig. 10. Measuring route A1–A2

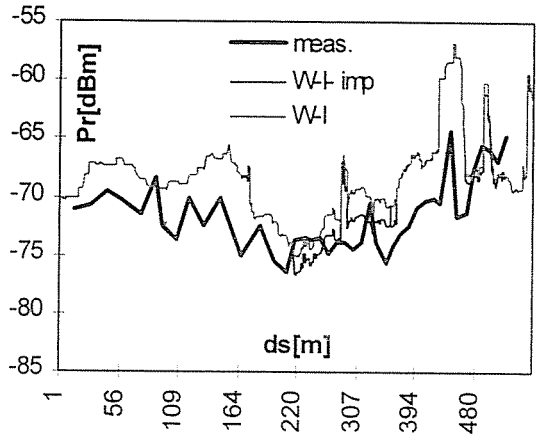

Fig. 11. Measuring route B1–B2

Fig. 9 with the aim of presenting the fluctuation of the building height, for which reason the test routes cannot be shown by this figure.

Fig. 10 – Fig. 13 show the received power level Pr versus the distance between the MS and the beginning of the measuring routes A1–A2 and B1–B2, ds.

The prediction curves W–I. and W–I.imp. given by *Fig. 10* and *Fig. 11* were obtained using digital database where the height of the buildings was also available (*Fig. 2*), while the curves W–I.AC. given by *Fig. 12* and *Fig. 13* represent the received power given by the COST 231 using an AutoCAD database containing only the value of the street width. For this

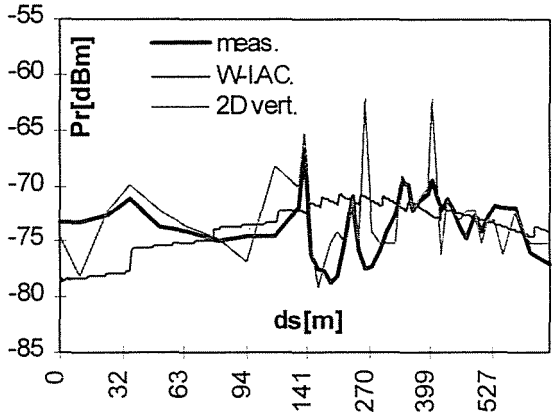

Fig. 12. Measuring route A1–A2

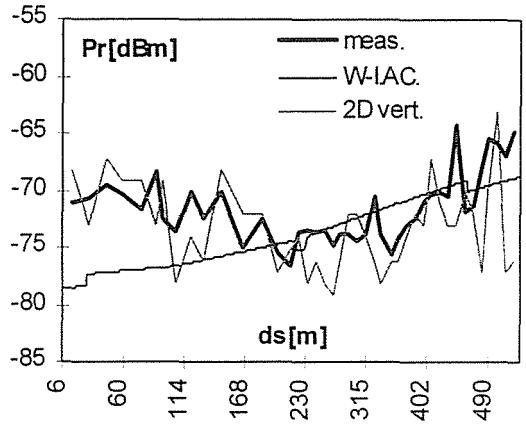

Fig. 13. Measuring route B1–B2

case the value of the building distance $b = 2 * w$ and a mean building height h_{roof}=26 m characteristic to the test area were used.

The divergence between the prediction and measurements in the middle of the route A1–A2 shown by *Fig. 10* is caused by the variable building distance along the radio path.

Table 3 shows the standard deviation of the predictions from the measurements. It can be observed from *Table 3* the effect of the modification of the model application and the dependence of the results on the used database.

Table 2
Table of standard deviations

	Model			
Route	W_I impr.	W_I	W_{IAC}	2D vert.
A1-A2	2.69	2.8	3.52	3.29
B1-B2	4.13	4.37	7.46	4.12
C1-C2	1.72	2.39	2.64	3.02
D1-D2	3.27	3.46	6.03	2.66

Table 3
Material parameters of a brick sample

Freq.[MHz]	Re(e)	Im(e)
400.00	2.753	0.407
450.00	2.638	0.450
500.00	2.640	0.449
600.00	2.600	0.605
700.00	2.583	0.837
800.00	2.724	0.995
900.00	2.791	1.079
1000.00	3.060	1.159
1200.00	3.499	1.224
1400.00	3.987	1.089
1600.00	4.405	0.817
1620.00	4.404	0.702
1650.00	4.448	0.609
1670.00	4.472	0.523
1700.00	4.632	0.420

The curves resulted from the comparison between measurements and prediction for routes C1–C2 ans D1–D2 are not presented because of the great number of the figures already included, but the standard deviation for these routes is also given by *Table 2.*

The results of the vertical plane model were also compared with the measurements and are shown by *Fig. 12* and *Fig. 13.* The comparison shows good agreement, but the differences become larger, when propagation on the street level should be taken into consideration. We plan to complete the model with the transverse plane, which will yield even better results.

Conclusion

In this paper the analysis of COST 231 Walfish–Ikegami model and a 3D model based on the UTD were presented.

In the first part of the paper the error introduced by the parameters of the COST 231 model, the effect of the database accuracy on the results and the modification in the application of the COST 231 model for the environment where the model assumptions are not satisfied were presented. The modification reduces the prediction errors to some degree but they still remain relative large because of the rough considerations of the COST 231 model. Therefore, a 3D model is going to be worked out from which the first results related to the vertical plane were presented in the second part of the paper. This model can already be used in the case when the BS antenna height is greater than the building height and it will be completed to be applicable on a larger scale of environments.

The predictions were assessed by measurements on an area of Budapest showing the applicability of the models.

Acknowledgement

The project is supported by the Hungarian National Scientific Research Fund (OTKA) under contract No. F015997. Special thanks are devoted to the Westel 900 Hungarian GSM service provider for making available the measurement results.

References

1. COST 231 TD (91) 73: Urban Transmission Loss Models for Mobile Radio in the 900 and 1800 MHz bands, The Hague, September, 1991.
2. WALFISH, J. – BERTONI, H. L.: A Theoretical Model of UHF Propagation in Urban Environments, *IEEE Trans. on AP*, Vol. 36, No. 12, 1988.
3. IKEGAMI, F. et al.: Propagation Factors Controlling Mean Field Strength on Urban Streets, *IEEE Trans. on AP*, Vol. 32, No. 8, 1984.
4. LOW, K.: Comparison of Urban Propagation Models with CW-Measurements, *IEEE VTC-92, Conference Record*, pp. 936–942 (1992).
5. NAGY, L. et al.: Comparison and Verification of Urban Propagation Models, *U.R.S.I. Int. Symp. On Elect. Th.*, St. Petersburg, May, 1995.
6. LEE, W. C. Y.: Mobile Celiular Telecommunication Systems, pp. 367–371. McGraw-Hill, 1989.
7. SÁNDOR, Z. – SZEKERES, B. – MARZA, E.: The Analysis of the COST 231 Walfish-Ikegami Model and a Comparison between Measurements and Prediction, received by the *Bul. Stiint. al Univers. din Timisoara*, 1995.
8. SÁNDOR, Z. – CSABA, T. – NAGY, L. – SZABÓ, Z.: Error Analysis and Improvement of the COST 231 Walfish-Ikegami Model and a Comparison between Measurements and Prediction, *4th Mobile and Personal Com. Sem.*, Limerick, June 1996.

9. CICHON, D. J. – KÜRNER, T. - WIESBECK, W.: Concepts and Results for 3D Digital Terrain Based Wave Propagation Models, An Overview, *IEEE Journal on Selected Areas in Communications*, Vol. 11, No.7, September 1993.
10. CICHON, D. J. – WIESBECK, W.: Ray Optical Wave Propagation Modeling in Urban Micro Cells, *IEEE, PIMRC'94*.
11. NAGY L.: An Improved TDR Method for Determining Material Parameters, *General Assembly of the International Union of Radio Science (URSI)*, Prague, 28 August-5 September 1990.

INDEX